Am. J. Hum. Genet. 63:1316–1328, 1998

Mutations of the Forkhead/Winged-Helix Gene, *FKHL7,* in Patients with Axenfeld-Rieger Anomaly

Alan J. Mears,[1,*] Tim Jordan,[2,*] Farideh Mirzayans,[1] Stéphane Dubois,[3] Tsutomu Kume,[4] Michael Parlee,[5] Robert Ritch,[6] Benjamin Koop,[5] Wen-Lin Kuo,[7] Colin Collins,[8] Jody Marshall,[1] Douglas B. Gould,[1] William Pearce,[1] Peter Carlsson,[9] Sven Enerbäck,[9] Jean Morissette,[3] Shomi Bhattacharya,[2] Brigid Hogan,[4] Vincent Raymond,[3] and Michael A. Walter[1]

[1]Departments of Ophthalmology and Medical Genetics, University of Alberta, Edmonton; [2]Department of Molecular Genetics, Institute of Ophthalmology, London; [3]Laboratory of Molecular Endocrinology, CHUL Research Center and Université Laval, Québec; [4]Howard Hughes Medical Institute, Vanderbilt University Medical Center, Nashville; [5]Centre for Environmental Health, Department of Biology, University of Victoria, Victoria, British Columbia; [6]Department of Ophthalmology, New York Eye and Ear Infirmary, New York; [7]Cancer Genetics Program, University of California, San Francisco; [8]Lawrence Berkeley National Laboratory, Berkeley; and [9]Department of Molecular Biology, Göteborg University, Göteborg

Summary

Genetic linkage, genome mismatch scanning, and analysis of patients with alterations of chromosome 6 have indicated that a major locus for development of the anterior segment of the eye, IRID1, is located at 6p25. Abnormalities of this locus lead to glaucoma. *FKHL7* (also called "*FREAC3*"), a member of the forkhead/winged-helix transcription-factor family, has also been mapped to 6p25. DNA sequencing of *FKHL7* in five IRID1 families and 16 sporadic patients with anterior-segment defects revealed three mutations: a 10-bp deletion predicted to cause a frameshift and premature protein truncation prior to the *FKHL7* forkhead DNA-binding domain, as well as two missense mutations of conserved amino acids within the *FKHL7* forkhead domain. *Mf1,* the murine homologue of *FKHL7,* is expressed in the developing brain, skeletal system, and eye, consistent with *FKHL7* having a role in ocular development. However, mutational screening and genetic-linkage analyses excluded *FKHL7* from underlying the anterior-segment disorders in two IRID1 families with linkage to 6p25. Our findings demonstrate that, although mutations of *FKHL7* result in anterior-segment defects and glaucoma in some patients, it is probable that at least one more locus involved in the regulation of eye development is also located at 6p25.

Received May 27, 1998; accepted for publication September 11, 1998; electronically published October 26, 1998.

Address for correspondence and reprints: Dr. Michael A. Walter, Ocular Genetics Laboratory, 832 Medical Sciences Building, University of Alberta, Edmonton, Alberta, Canada. E-mail: mwalter@gpu.srv.ualberta.ca

* These authors are co–first authors.

0002-9297/98/6305-0009$02.00

Introduction

Glaucoma is a major worldwide cause of blindness and is characterized by progressive degeneration of the optic nerve, usually associated with increased intraocular pressure (IOP). The Canadian National Institute for the Blind has identified glaucoma and macular degeneration as the two leading causes of blindness in Canada. Glaucoma is the primary cause of blindness in Canadians of African descent and is the second leading cause in Caucasians. It has been estimated that, by the year 2000, there will be ~67 million cases of glaucoma worldwide and almost 6.7 million cases of blindness as a direct result of the disease (Quigley 1996). More than 130,000 of these persons are estimated to become blind as a result of this glaucoma. Blindness from glaucoma usually begins with loss of peripheral vision. Central vision is often maintained until the late stages. By the time the patient notices visual loss, damage is advanced. In most cases, vision loss could have been prevented had glaucoma been detected and treated in time. Although glaucoma is as common as high blood pressure and diabetes, the general public lack of familiarity with it results in thousands of cases of blindness annually, most of which could have been prevented. The key to successful treatment lies in detection of glaucoma before irreversible optic-nerve damage has occurred.

Although a number of glaucoma genes have been mapped (Raymond 1997), only two glaucoma loci (*GLC1A* and *GLC3A*) have been cloned. A locus for primary open-angle glaucoma (*GLC1A*) was first mapped by genetic linkage analysis, in 1993, to markers on chromosome 1q21-1q31 (Sheffield et al. 1993). Stone and colleagues in early 1997 identified mutations in families with *GLC1A* in the *TIGR/myocilin* gene (Stone et al. 1997), a gene known previously to encode a trabecular meshwork protein postulated to have a role in the

regulation of IOP (Nguyen et al. 1993). To date, sequencing of the *TIGR/myocilin* gene in glaucoma patients (including unselected patients from walk-in glaucoma clinics) has indicated that ~4% of primary open-angle glaucoma patients have mutations in *TIGR/myocilin*. *GLC3A,* underlying rare autosomal recessive congenital glaucoma (OMIM 231300), has been mapped to 2p21 in a group of 17 families (Sarfarazi et al. 1995). Subsequently, mutations in the human cytochrome *P4501B1* gene were discovered in *GLC3A*-linked families (Stoilov et al. 1997).

Anterior-segment dysgenesis, the incorrect formation of the structures of the anterior segment of the eye, underlies some cases of congenital glaucoma (Kaiser-Kupfer 1989). Recently, several clinically related autosomal dominant disorders of anterior-segment formation that result in glaucoma have been genetically colocalized to chromosome 6p25. These disorders include iridogoniodysgenesis anomaly (IGDA; Mears et al. 1996; Graff et al. 1997), Axenfeld-Rieger anomaly (ARA; Gould et al. 1997), familial glaucoma iridogoniodysplasia (FGI; Jordan et al. 1997), and familial glaucoma with goniodysgenesis (FGG; Morissette et al. 1997). The results of genome mismatch–scanning studies have also indicated that a locus for anterior-segment dysgenesis is located at 6p25 (Mirzayans et al. 1997). Chromosomal alterations of 6p25 have also been reported in patients with a variety of clinical findings, including anterior-segment malformations and congenital glaucoma (Peeden et al. 1983; Reid et al. 1983; Levin et al. 1986; Zurcher et al. 1990; Alashari et al. 1995; Nishimura et al. 1997). The overlapping clinical presentations and colocalization of these disorders suggests that a single locus called "*IRID1*" (OMIM 601631), responsible for anterior-segment development and glaucoma, is located at 6p25. The glaucoma that *IRID1* patients develop is likely a result of incorrect regulation of the outflow of aqueous humor, because of the maldevelopment of the anterior segment–angle structures. Therefore, the *IRID1* locus is predicted to have a role in human eye development.

We report here the discovery of mutations in *IRID1* patients in *FKHL7,* a member of the evolutionarily conserved forkhead/winged-helix transcription-factor gene family. Expression studies and the eye phenotype of mouse embryos homozygous for null mutations of *Mf1,* the murine homologue of *FKHL7,* are consistent with a role for *Mf1*/*FKHL7* in eye development. However, mutation screening and genetic-linkage analyses have excluded *FKHL7* from underlying the glaucoma and anterior segment–dysgenesis phenotypes in two of the *IRID1* families with linkage to 6p25. Mutations of *FKHL7* were found only in ARA patients, suggesting that *FKHL7* underlies only the ARA phenotype of *IRID1*. It is probable that at least one additional locus involved in eye development must be located at 6p25.

Subjects, Material, and Methods

Clinical Data

The clinical presentations within *IRID1* families 1–5 have all been reported elsewhere. Families 1 and 2 were originally diagnosed with IGDA (Pearce et al. 1983; Mears et al. 1996), family 3 with ARA (Gould et al. 1997), family 4 with FGI (Jordan et al. 1997), and family 5 with FGG (Morissette et al. 1997). All five *IRID1* families demonstrate phenotypic variability, but affected individuals typically present with iris hypoplasia, iridocorneal angle defects (goniodysgenesis), and increased IOP with subsequent risk of glaucoma. Affected individuals within *IRID1* family 3 also had both a prominent, anteriorly displaced Schwalbe's line (posterior embryotoxon) attached to peripheral iris strands bridging the iridocorneal angle and displaced pupils (corectopia). Sixteen unrelated individuals with anterior-segment dysgenesis were also studied. The clinical findings in the five *IRID1* families and in the 16 additional individuals are presented in table 1. The study and collection of blood samples from all individuals included in the present report were approved by the Research Ethics Board of the Faculty of Medicine of the University of Alberta.

Polymorphic Markers

Novel polymorphisms were detected in exon 5 of the NAD(P)H:quinone oxidoreductase-2 gene (NQO2) by direct sequencing of PCR products amplified from key recombinant branches of the *IRID1* families. Primers for exon 5 were as follows: forward, 5′-gcttcattccgaatcaccag-3′; reverse, 5′-gtcccctccctccaactatc-3′. Primers were designed by use of *Primer 3,* available from the Primer3 Test Pre-Release (Whitehead Institute for Biomedical Research) Website. Each of the two polymorphisms within NQO2 exon 5 affects *Msp*I sites, at positions 111 bp and 188 bp of the 250-bp PCR product, generating a four-allele polymorphic system.

Physical Mapping

The preliminary physical map for the 6p25 *IRID1* region was obtained from the Whitehead Institute for BioMedical Research Web site. The human bacterial artificial chromosome (BAC) library (Shizuya et al. 1992; Kim et al. 1996) was screened by PCR with sequence-tagged sites (STSs)/expressed sequence tags (ESTs) mapped to the region, according to Research Genetics protocols. Selected clones were FISH mapped to confirm cytogenetic location and then were analyzed for STS content to determine order and overlap between clones.

Table 1

Clinical Features of Families and Patients in the Present Study

ID Number	Phenotype	Clinical Feature(s)[a]		Reference
		Ocular	Nonocular	
FAM1	IGDA	Abnormal angle vascularity, glaucoma, goniodysgenesis, iris hypoplasia	None	Mears et al. (1996)
FAM2	IGDA	Abnormal angle vascularity, glaucoma, goniodysgenesis, iris hypoplasia	None	Mears et al. (1996)
FAM3	ARA	Corectopia, glaucoma, goniodsygenesis, iris hypoplasia, iris strands, posterior embryotoxon	Deafness, heart anomalies	Gould et al. (1997)
FAM4		Glaucoma, goniodsygenesis, iris hypoplasia, Peter anomaly	None	Jordan et al. (1997)
FAM5	FGG	Glaucoma, goniodysgenesis, iris hypoplasia	None	Morissette et al. (1997)
UA patient 1	ARA	Glaucoma, iris hypoplasia	None	Present study
UA patient 2	ARA	Glaucoma, iris strands, posterior embryotoxin	None	Present study
UA patient 3	IGDA	Glaucoma, goniodsygenesis, iris hypoplasia	None	Present study
UA patient 4	ARA	Cataracts, glaucoma, goniodysgenesis, iris strands	None	Present study
UA patient 5	ARS	Glaucoma, Rieger eye malformation, sclerocornea	Dental anomalies	Present study
UA patient 6	ARS	Abnormal angle vascularity, glaucoma, iris hypoplasia, iris strands	Bowel resection, dental anomalies, inguinal hernia	Present study
UA patient 7	ARS	Cataracts, glaucoma, iris hypoplasia	Dental anomalies, mental retardation	Present study
UA patient 8	Anterior-segment dysgenesis	Cataracts, corectopia, iris hypoplasia, optic-nerve hypoplasia	None	Present study
UA patient 9	IGDA	Cataracts, goniodysgenesis	None	Present study
UA patient 10	ARS	Corectopia, glaucoma, iris strands, posterior embryotoxin	Dental anomalies, maxillary hypoplasia	Present study
UA patient 11	IGDA	Glaucoma, goniodysgenesis	None	Present study
UA patient 12	ARS	Cataracts, corectopia, glaucoma	Dental anomalies, maxillary hypoplasia, psychiatric illness	Present study
UA patient 13	IGDA	Glaucoma, goniodysgenesis, iris hypoplasia	None	Present study
UA patient 14	ARS	Corectopia, goniodysgenesis, glaucoma, iris hypoplasia, iris strands	dental anomalies	Present study
UA patient 15	ARA	Abnormal angle vascularity, corneal irregularities, glaucoma, iris strands	None	Present study
UA patient 16	ARA	Corectopia, glaucoma, goniodysgenesis, iris hypoplasia, iris strands	None	Present study

[a] Not every affected member of a family presented with all ocular or nonocular features listed for that family.

Sequence Scanning

Sequence scanning was performed on the BAC RMC06B016. This BAC, with an insert of ~150 kb, was sheared randomly, and fragments of 2–3 kb were subcloned into M13mp18 vector. Sequences were obtained from 509 subclones by ABI 373 and 377 automated sequencers and were assembled into contigs by Seqman (DNASTAR). Contigs were searched for coding sequence by BLAST 2.0 against the National Center for Biotechnology Information (GenBank) and dEST databases. GRAIL 1.2 was used to predict coding sequence not represented in existing databases.

Mutation Detection

Fragments were amplified from the single-exon *FKHL7* gene, by means of primers designed by *Primer3*. FKHL7 sequence has been deposited in Genbank (accession number AF078096). *FKHL7* primers are listed in table 2. PCR reactions were performed with 20 ng of DNA in a 25-μl volume containing 20 mM Tris-HCl (pH 8.4 at 23°C), 50 mM KCl, 1.5 mM $MgCl_2$, 200 μM each of dCTP, dTTP, dATP, and dGTP, and 60 ng of each primer. Dimethyl sulfoxide (final concentration 10%) was added to PCR reactions to alleviate secondary-structure problems created by the very high GC content of *FKHL7*. Each reaction was overlaid with 40 μl of light mineral oil to prevent evaporation. PCR specificity was increased through a "hot-start" step in which samples were subjected to a denaturing step of 5 min at 95°C, during which time 1 unit of *Taq* DNA polymerase and sufficient H_2O were added to produce a final total PCR-reaction volume of 25 μl. A further 3-min denaturing step at 95°C was followed by 35 cycles of denaturing at 94°C for 30 s, annealing at 58°C for 30 s, and extension at 72°C for 30 s, with a final elongation step of 72°C for 7 min. PCR products were purified with QIAquick columns (QIAGEN) and then were directly sequenced via ^{33}-P cycle sequencing (Amersham).

Mutations were confirmed in affected individuals and were screened for in 140 ethnically matched control chromosomes by the following methods: the 10-bp deletion (del nt 92–103) was detected through analysis of PCR products amplified with primer pair "C" on 1.5% agarose/1.5% NuSieve electrophoretic gels. The G245C mutation was detected through loss of an *Alu*I site in the PCR product amplified with primer set "D." The C261G mutation was detected through generation of a *Bsp*HI site in the PCR product amplified with primer set "B."

The insertion polymorphisms (GGC375ins and GGC347ins) were detected by sequencing in both patients and control individuals, by means of primer sets "H" and "I," respectively. PCR products using primer sets "H" and "I," containing the GGC375ins and GGC347ins polymorphisms, respectively, were separated on 6% denaturing polyacrylamide gels to obtain allele frequencies.

Expression Analysis

Expression of *FKHL7* was determined with commercially available northern blots (Clontech), with poly(A)$^+$-selected RNA from a variety of adult and fetal tissues. To avoid cross-hybridization with other forkhead-related genes, the probe for *FKHL7* was selected from the 3′ region (nucleotides 1192–1690). Hybridization and washes were performed according to the manufacturer's protocols. The human *β-ACTIN* control probe, provided by the manufacturer, was used to equalize loading differences. The methodologies of the expression studies using the $Mf1^{lacZ}$ allele of *Mf1*, the mouse *FKHL7* homologue, have been described in detail by Kume et al. (1998).

Results

Genetic Refinement of the Location of the IRID1 *Locus*

Genetic linkage analysis was used to refine the location of the *IRID1* locus. Analyses of new polymorphic loci

Table 2

Primer Pairs Used in PCR Amplification of *FKHL7*

Primer-Pair Designation	Primer (Nucleotide Position[a]) (5′→3′)		Product Size (bp)
	Forward	Reverse	
A	cccggactcggactcggc (−93 to −76)	ccgaggtagggcaccact (42 to 59)	152
B	gtccagccccaactccct (21 to 38)	cggctccttgaggtgc (567 to 582)	562
C	gtccagccccaactccct (21 to 38)	gcatggcggtgtagcc (106 to 121)	101
D	ggctacaccgccatgc (106 to 121)	actggtagatgccgttcagg (300 to 319)	214
E	ggcgcttcaagaagaaggac (515 to 535)	ctgaagccctggctatggt (908 to 926)	412
F	aagatcgagagccccgac (766 to 783)	cagaaggccggagctgag (982 to 999)	234
G	accatagccagggcttcag (908 to 926)	caggttgcagtggtaggtcc (1172 to 1191)	284
H	gagctccctctacagctccc (1071 to 1090)	gtgaccggaggcagagagta (1291 to 1310)	240
I	caagccatgagcctgtacg (1192 to 1210)	gggttcgatttagttcggct (1674 to 1693)	502

[a] Within the *FKHL7* gene of the primer; numbering is as in fig. 2.

that we generated (A. J. Mears and M. A. Walter, unpublished data), as well as the known 6p25 polymorphic markers in five *IRID1* families, were, overall, consistent with the localization of *IRID1* between D6S1600 and polymorphisms in the NQO2 gene (fig. 1). However, one unaffected individual (VIII:1 in *IRID1* family 1) had an apparent crossover event placing *IRID1* distal to D6S344 (fig. 1). This observation is inconsistent with *FKHL7* being a candidate gene for *IRID1* in family 1 (see below). The *IRID1* disease phenotype has been observed to be a fully penetrant autosomal dominant trait (Berg 1932; Weatherill and Hart 1969; Jerndal 1972; Mears et al. 1996; Gould et al. 1997; Jordan et al. 1997). Nevertheless, nonpenetrance of *IRID1* in individual VIII:1 in family 1 could not be formally ruled out as a possible explanation of this apparent mapping discrepancy.

FKHL7, *a Candidate Gene Located in the* IRID1 *Critical Region*

Twenty-nine BACs were obtained by screening a BAC genomic library with known STSs and ESTs to physically clone the *IRID1* interval (A. J. Mears and M. A. Walter, unpublished data). BAC RMC06B016 was found to contain the distal flanking marker D6S344 and to test positive with primers designed from published partial sequence of *FKHL7,* a gene previously mapped to 6p25 (Larsson et al. 1995). *FKHL7* is a member of the forkhead transcription-factor gene family shown to be involved in embryonic development, tissue-specific gene expression, and oncogenesis (Shapiro et al. 1993; Pierrou et al. 1994; Sasaki and Hogan 1994; Larsson et al. 1995; Kaufmann and Knochel 1996).

The DNA sequence of ~80% of BAC RMC06B016, or ~120 kb of sequence, was determined as a rapid means of both characterizing *FKHL7* and identifying additional genes within the *IRID1* critical region. The sequence of the forkhead-related region of BAC RMC06B016 was identical to the partial DNA sequence of the *FKHL7* gene (Larsson et al. 1995). Additional sequence analysis revealed that *FKHL7* has an intronless open-reading frame of 1,659 bp and is predicted to encode a protein of 553 amino acids (fig. 2). *Mf1,* the murine gene homologous to *FKHL7,* is also predicted to encode a protein 553 amino acids in length and has been mapped to mouse chromosome 13, in a region of conserved synteny with human 6p25 (Mouse Genome Informatics database). The human *FKHL7* gene and the mouse *Mf1* gene share 89% of their nucleotide sequence through the coding region, with the highest degree of

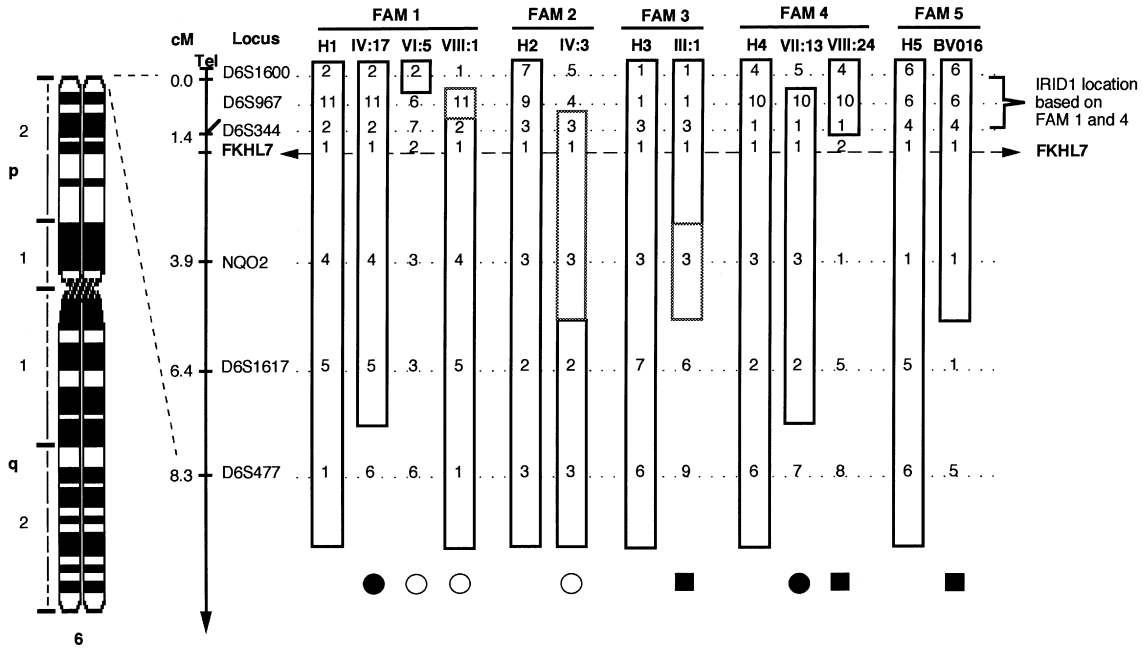

Figure 1 Genetic mapping of *IRID1* gene(s): schematic presentation of chromosome 6, illustrating the genetic mapping of the *IRID1* gene(s). Cumulative genetic distances (in cM) from the telomere are indicated on the left. The disease haplotypes segregating in each of the five *IRID1* families are labeled "H1"–"H5." For each locus, alleles were numbered according to size, from smallest to largest. Key recombinant individuals are identified at the top of the figure, with disease status indicated at the bottom. Square symbols indicate males, and circles indicate females. Boxed regions indicate the portion of the disease-associated haplotype present in the recombinant individual; stippled boxes indicate polymorphic loci for which haplotypes could not be unambiguously assigned. The location of the locus associated with anterior-segment dysgenesis and glaucoma in families 1 and 4 is indicated on the right.

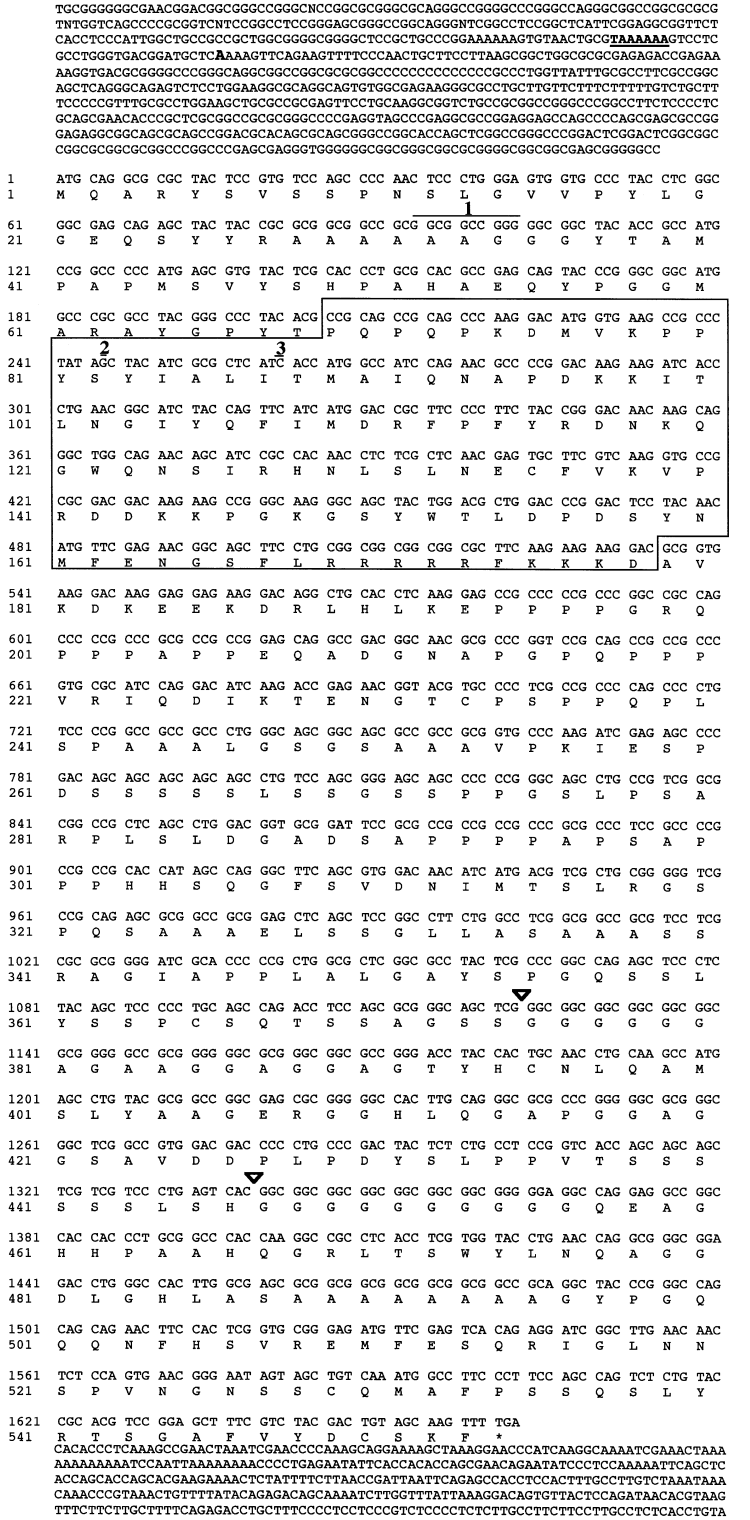

Figure 2 *FKHL7*, a member of the forkhead-domain family of transcription factors: nucleotide and predicted amino acid sequence of *FKHL7*. The open reading frame is 1,659 bp in length, predicted to encode a 553-amino-acid protein. The forkhead domain, spanning amino acids 69–178, is boxed. The best-predicted transcriptional start site, at position −526, is in boldface . The predicted TATA box, 25 bp farther upstream, is boldface and underlined. The arrowheads indicate the two locations of the polymorphic GGC insertions. The three *FKHL7* mutations detected in ARA patients are indicated by numerals "1"–"3." The horizontal bars above the nucleotide sequence denote the affected nucleotides. Mutation 1 is a 10-bp deletion of nucleotides 93–102, predicted to result in a frameshift coding alteration and premature protein truncation. Mutation 2 is G245C, resulting in the amino acid change Ser82Thr. Mutation 3 is C261G, resulting in the amino acid change Ile87Met.

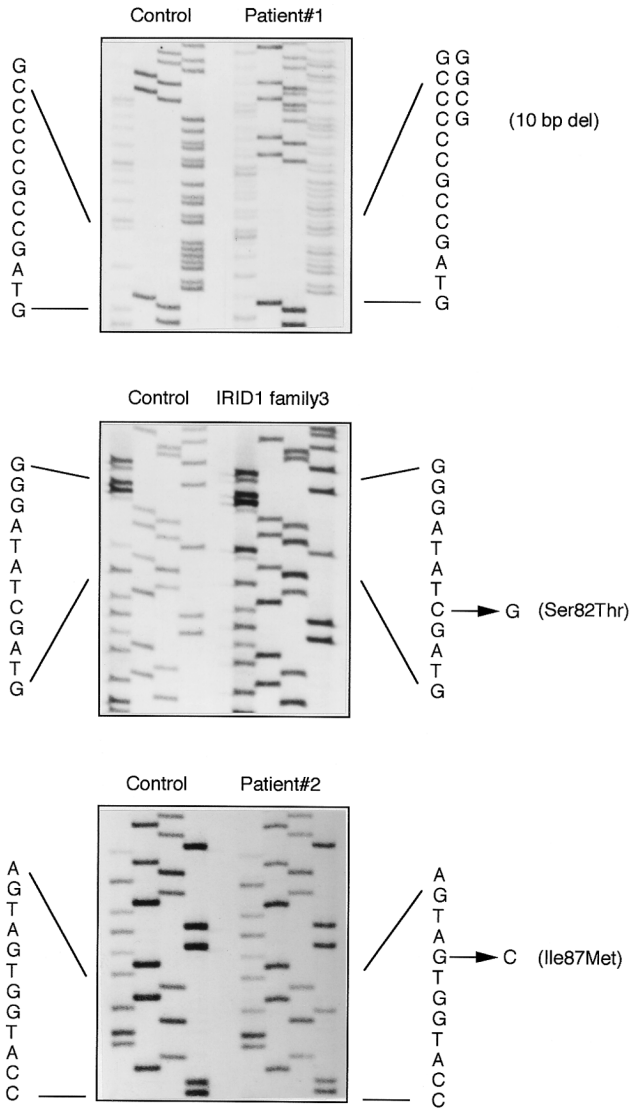

Figure 3 Sequence analysis of mutations of *FKHL7:* autoradiographs showing sequence analysis of the mutations identified in *IRID1* family 3 and in two sporadic patients with anterior-segment dysgenesis and glaucoma. PCR products were amplified from DNA samples from patients and were directly sequenced. Normal sequences are shown on the left; sequences from affected individuals are shown on the right. In each case, the reverse-primer sequence is shown, with the four lanes representing, from left to right, bases G, A, T, and C. The positions of the mutations are shown on the right. Predicted effects of *FKHL7* mutations are indicated on the far right.

identity (96%) seen over the 330 nucleotides of the forkhead domains. Overall, identity at the protein level was 92%, with 100% identity throughout the forkhead DNA-binding region. By use of an algorithm from the Promoter Prediction by Neural Network Website, a transcription start site has been predicted to occur at position −526, with aTATA box predicted 25 bp farther upstream (fig. 2). This predicted transcription start site is 32 bp upstream of the longest *Mf1* cDNA clone and is conserved between mice and humans.

FKHL7 *Mutations in Patients with Anterior Segment Dysgenesis and Glaucoma*

FKHL7 was screened for mutations by direct DNA sequencing of PCR products from affected individuals of the five *IRID1* families with linkage to 6p25 polymorphic loci and in 16 additional unrelated individuals with anterior-segment dysgenesis (table 1). Five nucleotide alterations in *FKHL7* were found (fig. 2). A 10-bp deletion, located between the initiation codon and the FKHL7 forkhead domain, was found in an individual with ARA and glaucoma (patient 1; fig. 3). This alteration is predicted to result in a frameshift mutation and premature stop after 10 amino acids and was not observed in >124 normal chromosomes. A second alteration, a G→C transversion at nucleotide position 245, predicted to result in a Ser82Thr mutation at the very beginning of helix 1 of the FKHL7 forkhead domain, was identified in *IRID1* family 3 (originally diagnosed with ARA; fig. 3). This G245C mutation abolishes an *Alu*I restriction-enzyme site and segregates with the anterior-segment dysgenesis/glaucoma phenotype in all affected members in family 3 (fig. 4). This G245C mutation was not observed in 140 normal chromosomes. This amino acid position is invariantly a serine in >80 forkhead-family genes over a range of species, from yeast to humans (Kaufmann and Knochel 1996). This serine is immediately adjacent to a conserved tyrosine amino acid residue that makes a phosphate-based contact with DNA (Clark et al. 1993). The distantly related *QRF1* (glutamine Q-rich factor 1) (Li and Tucker 1993) gene has a threonine instead of a serine residue at this position

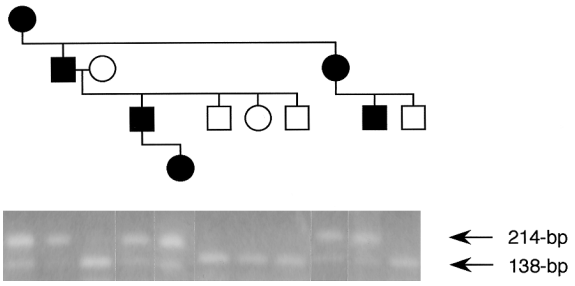

Figure 4 Segregation analysis of the G245C (Ser82Thr) mutation in *IRID1* family 3. Symbols designating affected and unaffected individuals and males and females are as in fig. 1. The 214-bp *FKHL7* amplification product generated from *FKHL7* primer pair "D" (table 2) is cleaved by *Alu*I into 138- and 76-bp fragments in unaffected individuals. The G245C mutation abolishes this *Alu*I site in affected individuals, and the resultant 214-bp allele segregates with the anterior segment–dysgenesis phenotype in *IRID1* family 3. The "normal" *Alu*I cleavage products present in affected individuals are generated from the nonmutated *FKHL7* allele in these individuals.

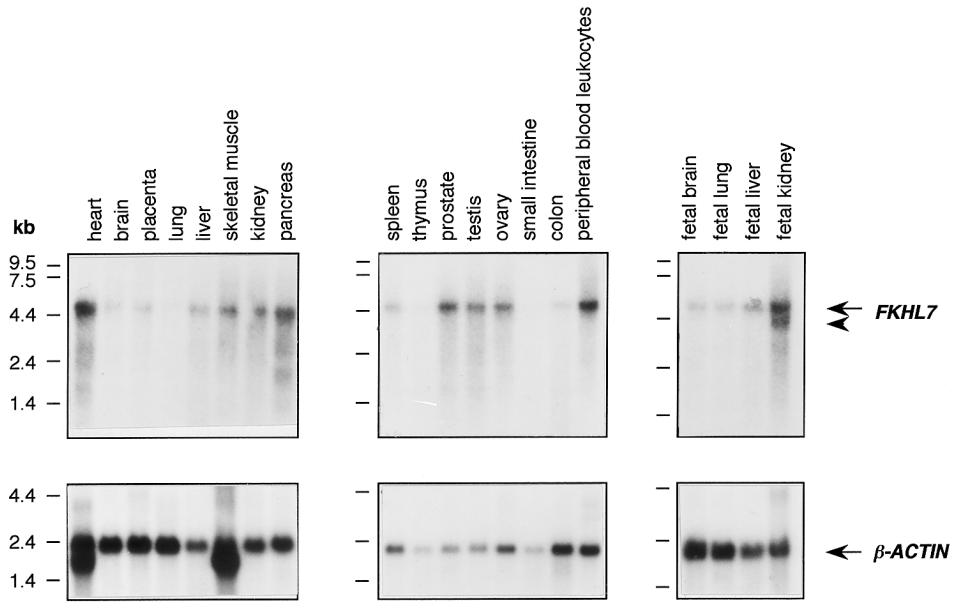

Figure 5 Northern blot analysis of *FKHL7:* expression in human tissues. A commercial multiple-tissue northern blot was hybridized with a *FKHL7* probe (*upper panels*) and with a *β-ACTIN* control probe (*lower panels*). The 4.5-kb *FKHL7* transcript is indicated by an arrow, on the right. A 4.0-kb alternative *FKHL7* transcript is also present in fetal kidney RNA and is indicated by an arrowhead.

at the start of helix 1. However, since the QRF1 DNA-binding domain is only 84 amino acids in length, compared with 110 amino acids for all other known forkhead proteins, QRF1 could well fall outside the forkhead family. Consistent with this notion, QRF1 appears to bind DNA differently from the manner that is predicted for forkhead proteins (Clark et al. 1993; Li and Tucker 1993) and therefore may not require a serine at this position. Site-directed mutagenesis of both this serine and the two flanking tyrosines in the related forkhead gene *HNF-3γ* abolished DNA-binding activity (Clevidence et al. 1993). The third mutation, a C→G transversion at nucleotide position 261, which would result in the missense mutation Ile87Met in helix 1 of the FKHL7 forkhead domain (fig. 2), was identified in an individual diagnosed with ARA and glaucoma (patient 2; fig. 3). This C261G mutation creates a *Bsp*HI restriction-enzyme site. This mutation was not observed in 144 normal chromosomes. This position within helix 1 is an isoleucine in >88% of forkhead genes and has never been reported as a methionine (Kaufmann and Knochel 1996). Interestingly, as well as occurring within the putative DNA-binding domain of FKHL7, both the Ser82Thr and the Ile87Met missense mutations occur within a conserved region proposed to act as a nuclear-localization signal necessary and sufficient for nuclear targeting of the related forkhead-family gene, *HNF-3β* (Qian and Costa 1995).

Two alterations, GGC375ins and GGC447ins, each involving the insertion of an extra GGC triplet in two separate GGC repeats within the *FKHL7* coding region (fig. 2), were found both in patients and in control individuals. These alterations are therefore presumed to be non-*IRID1*–associated polymorphisms of *FKHL7*. GGC375ins has two alleles; 77% of 94 normal control chromosomes are observed to carry the GGC_6 allele, 23% the GGC_7 allele. The GGC447ins polymorphism also has two alleles; 83% of 110 normal control chromosomes are observed to carry the GGC_7 allele, 17% the GGC_8 allele. Although the GGC repeat associated with the human GGC375ins polymorphism is conserved in the mouse *Mf1* sequence, there is no evidence that the murine GGC repeat is polymorphic.

FKHL7 *Expression Studies*

A 4.5-kb *FKHL7* mRNA transcript was detected by northern blot analyses in multiple adult and fetal human tissues. Highest expression of *FKHL7* was observed in adult kidney, heart, peripheral blood leukocytes, and prostate and in fetal kidney (fig. 5). An alternative transcript of size 4.0 kb was also detected in fetal kidney, possibly suggesting use of an alternate promoter or polyadenylation site in this tissue. This *FKHL7* fetal-kidney alternative transcript has also been observed in previous studies (Pierrou et al. 1994; Nishimura et al. 1998). PCR analyses indicated that *FKHL7* was also expressed in human fetal craniofacial RNA and in the adult iris (data not shown).

The murine *Mf1* gene was inactivated by homologous

recombination in embryonic stem cells in which sequences corresponding to amino acids 50–553 and the 3′ UTR of the *Mf1* gene were replaced by a lacZ/PGKneo^r cassette in frame with the first AUG (Kume et al. 1998). Mf1^{lacZ}-homozygous mice developed severe eye anomalies and hydrocephalus (Kume et al. 1998). LacZ activity was analyzed in Mf1^{lacZ}-homozygous and -heterozygous embryos to analyze *Mf1* expression in more detail. In the eye of 14.5 dpc heterozygous and homozygous mouse embryos, lacZ staining was abundant in the periocular mesenchyme and in the developing lids and anterior segment of the eye (fig. 6). *Mf1* is widely expressed in mesenchyme tissues and in the developing eye (Kume et al. 1998). Both the expression pattern of the murine homologue of the *FKHL7* gene and the fact that *Mf1*-homozygous-null mutant mouse embryos have severe eye findings in addition to hydrocephalus are strongly consistent with the hypothesis that *FKHL7* has a role in eye development. The relatively less severe anomalies observed in human *IRID1* patients compared with the *Mf1* homozygous mutant mice presumably result from the fact that *IRID1* patients are heterozygotes and thus retain a single functional copy of the *FKHL7* gene.

IRID1: *Genetically Heterogeneous*

Surprisingly, complete DNA sequencing of the *FKHL7*-gene coding region in affected individuals of families 1, 2, 4, and 5 failed to identify any additional *IRID1*-associated mutations of *FKHL7*. Although the high GC content of *FKHL7* makes it remotely possible that a *FKHL7* mutation could be missed because of GC compressions despite our efforts to resolve the *FKHL7* sequence, it is very unlikely that mutations in all four families would be missed. In addition, analysis of the GGC447ins polymorphism in *IRID1* family 4 genetically excluded the *FKHL7* gene from underlying the *IRID1* phenotype in this family (fig. 1). Since the GGC447ins polymorphism is only 1,341 bp from the translation start, and since *FKHL7* does not contain any introns, it is exceedingly unlikely that an intragenic crossover event could explain these findings. Instead, the recombination event in VIII:24 of *IRID1* family 4, together with the recombination event within unaffected individual VIII:1 in *IRID1* family 1, discussed above, is strongly consistent with the localization, between D6S1600 and D6S344, of a second locus associated with anterior-segment dysgenesis and glaucoma (fig. 1).

Discussion

There is increasing genetic evidence that members of the forkhead/winged-helix gene family play key roles in embryonic development, cell-fate determination, and tissue-specific gene expression, in both vertebrates and invertebrates (Kaufmann and Knochel 1996). For example, the prototypic *forkhead* (*fkh*) gene of *Drosophila* regulates fore and hindgut development and morphogenesis and controls the localized expression of signaling genes such as *wingless* (*wg*), *hedgehog* (*hh*), and *decapentaplegic* (*dpp*) (Weigel et al. 1989; Hoch and Pankratz 1996). Aspects of this role of *fkh* in gut development appear to have been conserved during evolution (Roberts et al. 1995). In mammals, mutation of the *winged-helix nude* (*whn*) forkhead gene disrupts normal hair growth and thymus development in nude mice and rats (Nehls et al. 1994), whereas mice with loss-of-function mutations of the forkhead gene *HNF-3β* exhibit defects in notochord and gut formation (Ang and Rossant 1994; Weinstein et al. 1994).

Forkhead-family genes have also been implicated in tumorigenesis. The forkhead-related avian sarcoma virus 31 gene, *qin,* determines the transforming ability of the retrovirus (Li and Vogt 1993). Translocations between chromosomes 2 and 13 that fuse the *PAX3* gene to the forkhead gene *FKHR* have been found in pediatric alveolar rhabdomyosarcoma (Galili et al. 1993). Fusion of the zinc-finger transcription gene HTRX1 on chromosome 11 to the AFX1 forkhead gene on the X chromosome have also been found in acute lymphocytic leukemia patients with t(X,11) translocations (Parry et al. 1994).

While this study was under review, *FKHL7* was reported to be (*a*) located <20 kb from the 6p25 translocation breakpoint in an individual with an unbalanced, t(2,6)(q35, p25) karyotype who presented with a variety of clinical findings including glaucoma and (*b*) mutated in four small families with anterior segment–dysgenesis phenotypes (Nishimura et al. 1998). Our finding of *FKHL7* mutations in three patients with ocular defects confirms these findings and implicates *FKHL7* in ARA. The 10-bp deletion of the *FKHL7* gene is predicted to result in a frameshift and truncated protein, whereas the two missense mutations of highly conserved amino acids could impair DNA binding and, possibly, nuclear localization of the FKHL7 protein. Although northern blot–expression studies have found that *FKHL7* is widely expressed in adult and fetal tissues, the expression of *Mf1* in the mesenchyme of the developing eye is very similar to that observed for the *RIEG/PITX2* gene. *RIEG* mutations result in Axenfeld-Rieger syndrome (ARS), an autosomal dominant disorder presenting with ARA-like ocular findings in addition to abnormalities of the teeth, jaw, and umbilicus (Semina et al. 1996). The three presumed inactivating mutations of *FKHL7* and the expression pattern of *Mf1* in the developing eye are consistent with haploinsufficiency of *FKHL7* as underlying the autosomal dominant glaucoma and anterior-segment dysgenesis in our ARA patients. Interestingly,

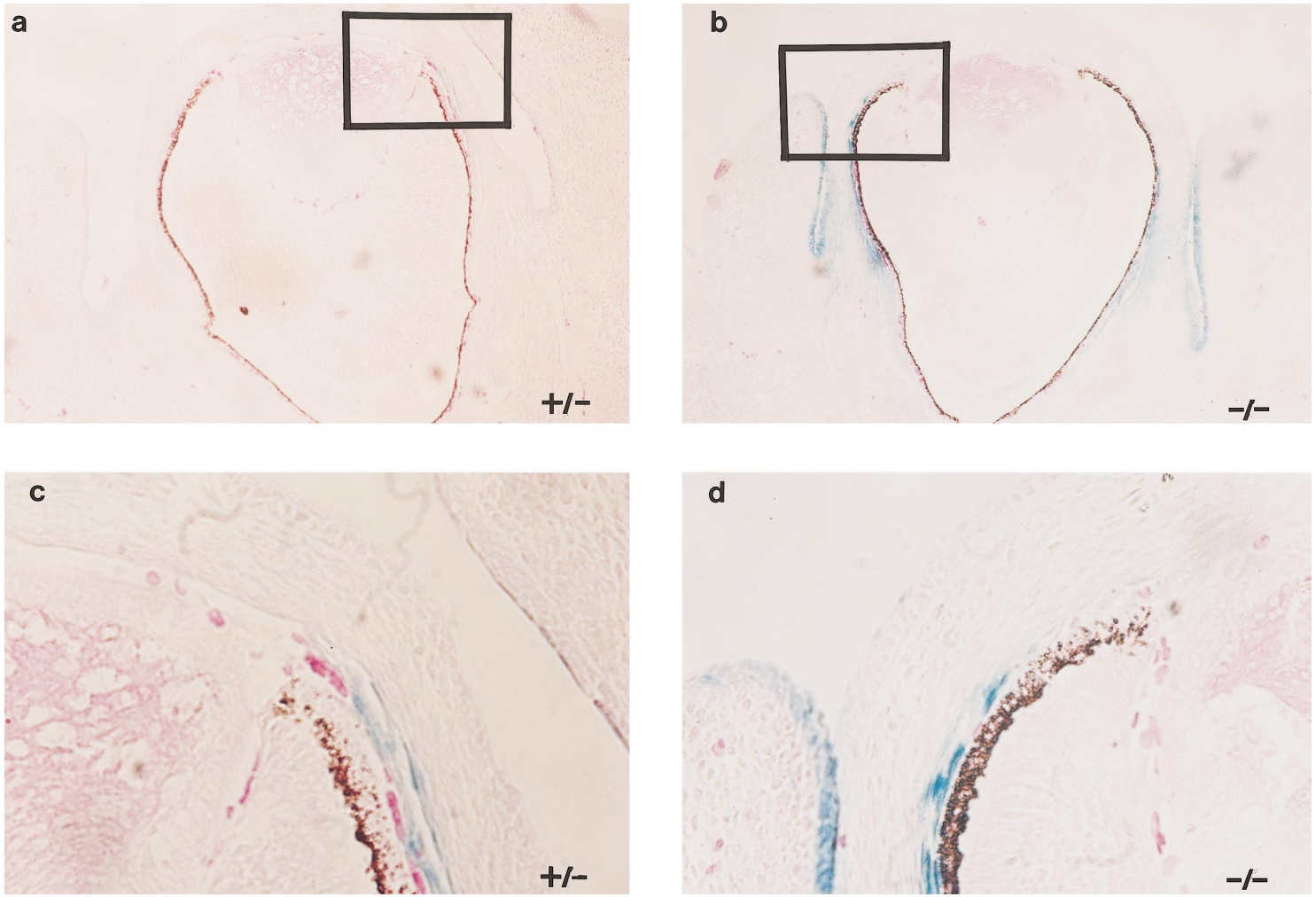

Figure 6 Expression studies of the *FKHL7* mouse homologue *Mf1*. A *Mf1* knockout mouse was generated by homologous recombination in embryonic stem cells in which sequences corresponding to amino acids 50–553 and the 3′ UTR of the *Mf1* gene were replaced by a lacZ/PGKneo^r cassette in frame with the first AUG (Kume et al. 1998). *Mf1* expression in *Mf1*lacZ/+ (+/−) and *Mf1*lacZ/*Mf1*lacZ (−/−) embryos are indicated by the lacZ staining observed in photographs of sections of the developing eye in 14.5 dpc mice. The boxed regions in panels *a* and *b* are shown magnified in panels *c* and *d*, respectively. Blue-stained tissue indicates regions of lacZ expression, corresponding to abundant *Mf1* expression in the periocular mesenchyme, developing lids, and anterior segment.

aniridia (i.e., partial to complete absence of the iris plus abnormalities of the cornea, lens, and retina) and ARS, both of which are autosomal dominant anterior-segment malformations, also result from haploinsufficiency of the *PAX6* and *RIEG* transcription factors, respectively (Glaser et al. 1992; Jordan et al. 1992; Hanson et al. 1993; Semina et al. 1996). Anterior-segment formation must therefore be under extremely stringent transcriptional control.

Interestingly, all three mutations found here in the *FKHL7* gene occurred in patients originally diagnosed with the ARA form of *IRID1*. The four additional *FKHL7* mutations recently reported by Nishimura et al. (1998) also occurred in ARA individuals. To date, only 20%–30% of ARA/ARS patients have been found to have mutations in the *RIEG* gene at chromosome 4q25 (S. Kulak and M. A. Walter, unpublished data). A significant portion of ARS patients might therefore have mutations of *FKHL7* instead. ARS type 2 (*RIEG2;* anterior-segment anomalies plus nonocular features) has been mapped to 13q14 (Phillips et al. 1996), the location of the forkhead gene, *FKHR*. This gene must therefore be considered an excellent candidate for *RIEG2*.

Mutational screening, however, excluded *FKHL7* from underlying the anterior-segment disorders in four families with glaucoma and anterior-segment dysgenesis linked to 6p25. Genetic-linkage analyses using a GGC trinucleotide–repeat polymorphism found within both the *FKHL7* coding region (fig. 2) and nearby polymorphic loci also excluded the *FKHL7* gene in two of these families (fig. 1). Interestingly, these four families—*IRID1* families 1, 2, 4, and 5—were originally diagnosed with IGDA, IGDA, FGI, and FGG, respectively. The *FKHL7* mutations that we found occurred in a family and in two sporadic patients all originally diagnosed with ARA. Although all these autosomal dominant disorders include glaucoma, iris hypoplasia, and anterior-angle defects, ARA patients additionally present with a prominent, anteriorly displaced Schwalbe's line attached to peripheral iris strands bridging the iridocorneal angle and displaced pupils, features not typically seen in IGDA, FGI, or FGG. The four remaining *IRID1* families might thus be phenotypically as well as genetically distinct from the ARA family and patients found to carry *FKHL7* mutations. Precluding intragenic crossover in these families and the unlikely possibility that mutations of noncoding portions of *FKHL7* underlying *IRID1* in all four remaining glaucoma and anterior segment–dysgenesis families, at least one additional locus involved in the regulation of eye development must be located at 6p25.

Note added in proof.—After this article was accepted for publication, additional information came to our attention, indicating that mice heterozygous for an inactivating allele of *Mf1* display anterior-segment anomalies including an absent or small Schlemm's canal and hypoplastic trabecular meshwork (S. John, personal communication), strongly supporting the hypothesis that *FKHL7/Mf1* has a significant role in eye development.

Acknowledgments

We would like to express our gratitude to the *IRID1* families and patients for their cooperation and enthusiasm for this project. We thank the members of the Departments of Medical Genetics and Ophthalmology, University of Alberta, for critical comments on this research and the manuscript. We also would like to thank K. McElligott, J. Schmidt, and S. Christian for their excellent coordination of patient resources. A large number of ophthalmologists participated in this study. We are particularly indebted to Mr. Erich Weber (Austria) for referral of patients. This research was funded by Alberta Heritage Fund for Medical Research (AHFMR) grant EG9400216, the Canadian Genetic Diseases Network, and Medical Research Council of Canada (MRC) grant MT12916 to M.A.W. and, partly, by MRC grant MA13428 to V.R. D.B.G. is a University of Alberta 75th Anniversary Award Scholar. V.R. is a "chercheur-boursier clinicien," of the Fonds de la Recherche en Santé du Québec. M.A.W. is an MRC and AHFMR scholar. A.J.M. is funded by an AHFMR postdoctoral fellowship. T.J. is supported by Wellsome Trust grant 04361/z/94.

Electronic-Database Information

BLAST (National Center for Biotechnology Information), http://www.ncbi.nlm.nih.gov/BLAST (for BLAST2 and EST databases)

Mouse Genome Informatics (The Jackson Laboratory), http://www.informatics.jax.org/

National Center for Biotechnology Information (GenBank), http://www.ncbi.nlm.nih.gov/genbank/query_form.html

Online Mendelian Inheritance in Man (OMIM), http://www/ncbi.nim.nih.gov/omim (for clinical phenotypes and linkage dataAxenfeld-Rieger syndrome, ARA, IGDA, iridogoniodsgenesis syndrome, and IRID1)

Primer3 Test Pre-Release (Whitehead Institute for BioMedical Research), http://www-genome.wi.mit.edu/cgi-bin/primer/primer3.cgi

Promoter Prediction by Neural Network (Lawrence Berkeley National Laboratory), http://www-hgc.lbl.gov/projects/promoter.html

References

Alashari M, Chen E, Poskanzer L (1995) Partial deletion of chromosome 6p: autopsy findings in a premature infant and review of the literature. Pediatr Pathol Lab Med 15:941–947

Ang SL, Rossant J (1994) HNF-3 beta is essential for node and notochord formation in mouse development. Cell 78: 561–574

Berg F (1932) Erbliches jugendliches Glaukom. Acta Ophthal 10:568–587

Clark KL, Halay ED, Lai E, Burley SK (1993) Co-crystal struc-

ture of the HNF-3/fork head DNA-recognition motif resembles histone H5. Nature 364:412–420

Clevidence DE, Overdier DG, Tao W, Qian X, Pani L, Lai E, Costa RH (1993) Identification of nine tissue-specific transcription factors of the hepatocyte nuclear factor 3/forkhead DNA-binding-domain family. Proc Natl Acad Sci USA 90: 3948–3952

Galili N, Davis RJ, Fredericks WJ, Mukhopadhyay S, Rauscher FD, Emanuel BS, Rovera G, et al (1993) Fusion of a fork head domain gene to PAX3 in the solid tumour alveolar rhabdomyosarcoma. Nat Genet 5:230–235

Glaser T, Walton DS, Maas RL (1992) Genomic structure, evolutionary conservation and aniridia mutations in the human pax6 gene. Nat Genet 2:232–239

Gould DB, Mears AJ, Pearce WG, Walter MA (1997) Autosomal dominant Axenfeld-Rieger anomaly maps to 6p25. Am J Hum Genet 61:765–768

Graff C, Jerndal T, Wadelius C (1997) Fine mapping of the gene for autosomal dominant juvenile-onset glaucoma with iridogoniodysgenesis in 6p25-tel. Hum Genet 101:130–134

Hanson IM, Seawright A, Hardman K, Hodgson S, Zaletayev D, Fekete G, van Heyningen V (1993) PAX6 mutations in aniridia. Hum Mol Genet 2:915–920

Hoch M, Pankratz MJ (1996) Control of gut development by fork head and cell signaling molecules in Drosophila. Mech Dev 58:3–14

Jerndal T (1972) Dominant goniodysgenesis with late congenital glaucoma: a re-examination of Berg's pedigree. Am J Ophthalmol 74:28–33

Jordan T, Ebenezer N, Manners R, McGill J, Bhattacharya S (1997) Familial glaucoma iridogoniodysplasia maps to a 6p25 region implicated in primary congenital glaucoma and iridogoniodysgenesis anomaly. Am J Hum Genet 61: 882–888

Jordan T, Hanson I, Zaletayev D, Hodgson S, Prosser J, Seawright A, Hastie N, et al (1992) The human PAX6 gene is mutated in two patients with aniridia. Nat Genet 1:328–332

Kaiser-Kupfer MI (1989) Neural crest origin of trabecular meshwork and other structures of the anterior chamber. Am J Ophthalmol 107:671–673

Kaufmann E, Knochel W (1996) Five years on the wings of fork head. Mech Dev 57:3–20

Kim U-J, Birren B, Slepak T, Mancino V, Boysen C, Kang HL, Simon MI, et al (1996) Construction and characterization of a human bacterial artificial chromosome library. Genomics 34:213–218

Kume T, Deng K-Y, Winfrey V, Gould DB, Walter MA, Hogan BLM (1998) The forkhead/winged helix gene Mf1 is disrupted in the pleiotropic mouse mutation congenital hydrocephalus. Cell 93:985–996

Larsson C, Hellqvist M, Pierrou S, White I, Enerbäck S, Carlsson P (1995) Chromosomal localization of six human forkhead genes, freac-1 (FKHL5), -3 (FKHL7), -4 (FKHL8), -5 (FKHL9), -6 (FKHL10), and -8 (FKHL12). Genomics 30: 464–469

Levin H, Ritch R, Barathur R, Dunn MW, Teekhasaenee C, Margolis S (1986) Aniridia, congenital glaucoma, and hydrocephalus in a male infant with ring chromosome 6. Am J Med Genet 25:281–287

Li C, Tucker PW (1993) DNA-binding properties and secondary structure model of the hepatocyte nuclear factor 3/fork head domain. Proc Natl Acad Sci USA 90:11583–11587

Li J, Vogt PK (1993) The retroviral oncogene qin belongs to the transcription factor family that includes the homeotic gene fork head. Proc Natl Acad Sci USA 90:4490–4494

Mears AJ, Mirzayans F, Gould DB, Pearce WG, Walter MA (1996) Autosomal dominant iridogoniodysgenesis anomaly maps to 6p25. Am J Hum Genet 59:1321–1327

Mirzayans F, Mears AJ, Gou S-W, Pearce WG, Walter MA (1997) Isolation of the chromosomal region containing the iridogoniodsygenesis anomaly locus by genomic mismatch scanning. Am J Hum Genet 61:111–119

Morissette J, Falardeau P, Dubois S, Bergeron J, Vonvk P, Cote G, Anctil J-P, et al (1997) A common gene for developmental and familial open-angle glaucomas confined on chromosome 6p25. Am J Hum Genet Suppl 61:A286

Nehls M, Pfeifer D, Schorpp M, Hedrich H, Boehm T (1994) New member of the winged-helix protien family disrupted in mouse and rat nude mutations. Nature 372:103–107

Nguyen TD, Huang W, Bloom E, Polansky JR (1993) Glucocorticoid effects on HTM cells: molecular biology approaches. In: Lütjen-Drecoll E (ed) Basic aspects of glaucoma research. Vol 3. Schattauer & Stuggart, New York, pp 331–343

Nishimura DY, Alward WLM, Beck G, Hockey R, Patil S, Stone EM, Sheffield VC (1997) Characterization of 6p25 chromosomal anomalies in two patients identifies a potential candidate gene causing congenital glaucoma. Am J Hum Genet Suppl 61:A21

Nishimura DY, Swiderski RE, Alwards LM, Searby CC, Patil SR, Bennet SR, Kanis AB, et al (1998) The forkhead transcription factor gene FKHL7 is responsible for glaucoma phenotypes which map to 6p25. Nat Genet 19:140–147

Parry P, Wei Y, Evans G (1994) Cloning and characterization of the t(X;11) breakpoint from a leukemic cell line identify a new member of the forkhead gene family. Genes Chromosom Cancer 11:79–84

Pearce WG, Wyatt HT, Boyd TAS, Ombres RS, Salter AB (1983) Autosomal dominant iridogoniodysgenesis: genetic features. Can J Ophthalmol 18:7–10

Peeden JN, Scarbrough P, Taysi K, Wilroy RS, Finley F, Luthardt F, Martens P, et al (1983) Ring chromosome 6: variability in phenotypic expression. Am J Med Genet 16: 563–573

Phillips JC, Del Bono EA, Haines JL, Pralea AM, Cohen JS, Greff LJ, Wiggs JL (1996) A second locus for Rieger syndrome maps to chromosome 13q14. Am J Hum Genet 59: 613–619

Pierrou S, Hellqvist M, Samuelsson L, Enerback S, Carlsson P (1994) Cloning and characterization of seven human forkhead proteins: binding site specificity and DNA bending. EMBO J 13:5002–5012

Qian X, Costa RH (1995) Analysis of hepatocyte nuclear factor-3β protein domains required for transcriptional activation and nuclear targeting. Nucleic Acids Res 23:1184–1191

Quigley HA (1996) Number of people with glaucoma worldwide. Br J Ophthalmol 80:389–393

Raymond V (1997) Molecular genetics of glaucomas: mapping of the first five "GLC" loci. Am J Hum Genet 60:272–277

Reid CS, Stamberg J, Phillips JA (1983) Monosomy for distal

segment 6p: clinical description and use in localizing a region important for expression of Hageman factor. Pediatr Res Suppl 17:217A

Roberts DJ, Johnson RL, Burke AC, Nelson CE, Morgan BA, Tabin C (1995) Sonic hedgehog is an endodermal signal inducing Bmp-4 and Hox genes during induction and regionalization of the chick hindgut. Development 121: 3163–3174

Sarfarazi M, Akarsu AN, Hossain A, Turacli ME, Aktan SG, Barsoum HM, Chevrette L, et al (1995) Assignment of a locus (GLC3A) for primary congenital glaucoma (buphthalmos) to 2p21 and evidence for genetic heterogeneity. Genomics 30:171–177

Sasaki H, Hogan B (1994) Hnf-3-beta as a regulator of floor plate development. Cell 76:103–115

Semina EV, Reiter R, Leysens NJ, Alward WL, Small KW, Datson NA, Siegel BJ, et al (1996) Cloning and characterization of a novel bicoid-related homeobox transcription factor gene, RIEG, involved in Rieger syndrome. Nat Genet 14:392–399

Shapiro DN, Sublett JE, Li BT, Downing JR, Naeve CW (1993) Fusion of pax3 to a member of the forkhead family of transcription factors in human alveolar rhabdomyosarcoma. Cancer Res 53:5108–5112

Sheffield VC, Stone EM, Alward WLM, Drack AV, Johnson AT, Streb LM, Nichols BE (1993) Genetic-linkage of familial open-angle glaucoma to chromosome 1q21-q31. Nat Genet 4:47–50

Shizuya H, Birren B, Kim U-J, Mancino V, Slepak T, Tachiiri Y, Simon M (1992) Cloning and stable maintenance of 300-kilobase-pair fragments of human DNA in Escherichia coli using an F-factor based vector. Proc Natl Acad Sci USA 89: 8794–8797

Stoilov I, Akarsu AN, Sarfarazi M (1997) Identification of three different truncating mutations in cytochrome P4501B1 (CYP1B1) as the principal cause of primary congenital glaucoma (buphthalmos) in families linked to the GLC3A locus on chromosome 2p21. Hum Mol Genet 6:641–647

Stone EM, Fingert JH, Alward WLM, Nguyen TD, Polansky JR, Sunden SLF, Nishmura D, et al (1997) Identification of a gene that causes primary open angle glaucoma. Science 275:668–670

Weatherill JR, Hart CT (1969) Familial hypoplasia of the iris stroma associated with glaucoma. Br J Ophthalmol 53: 433–438

Weigel D, Jurgens G, Kuttner F, Seifert E, Jackle H (1989) The homeotic gene *fork head* encodes a nucelar protein and is expressed in the terminal regions of the Drosophila embryo. Cell 57:645–658

Weinstein DC, Ruiz I, Altaba A, Chen WS, Hoodless P, Prezioso VR, Jessell TM, et al (1994) The winged-helix transcription factor HNF-3β is required for notochord development in the mouse embryo. Cell 78:575–588

Zurcher VL, Golden WL, Zinn AB (1990) Distal deletion of the short arm of chromosome 6. Am J Med Genet 35: 261–265